I*($^2P_{1/2}$) and Cl*($^2P_{1/2}$) Production from Chloroiodobenzenes in the Ultraviolet[†]

Dulal Senapati, Sandip Maity, and Puspendu K. Das*

Department of Inorganic and Physical Chemistry, Indian Institute of Science, Bangalore-560012, India

Received: February 13, 2004; In Final Form: May 31, 2004

The relative quantum yields of I*($^2P_{1/2}$) and Cl*($^2P_{1/2}$) production, ϕ*(I) and ϕ*(Cl), respectively, have been measured at four different ultraviolet excitation wavelengths, e.g., 222, 236, 266, and 280 nm in the photodissociation of *o*-, *m*-, and *p*-chloroiodobenzenes. The measured I* and Cl* quantum yields are, with some exceptions, higher than those obtained, respectively, from iodobenzene and chlorobenzene, at the same wavelengths. While at most wavelengths the major fraction of the iodine atoms is produced in the excited state, the opposite is true for the chlorine atoms. Both direct and indirect dissociation pathways are involved in the production of I* atoms whereas Cl* is produced only by indirect pathways since direct excitation of the σ*(C−Cl) ← n(Cl) transition is not possible at these wavelengths. The halogen atom in the ortho position is found to be most effective in enhancing the yield of the other spin−orbit excited halogen atom in the photolysis. While the nature of the initial transition, the extent of intersystem crossing in the excited states and the exit channel effects need to be considered in interpreting the quantum yield results, some factors seem to be more effective in influencing the final outcome. Induced dipole−induced dipole and quadrupole−quadrupole interactions between the two halogen atoms (I and Cl in this case) seem to play an important role in the exit channel dynamics. These electrostatic interactions facilitate the intersystem transfer in the excited state and subsequent production of the spin−orbit excited halogen atoms.

1. Introduction

Like alkyl and aryl monohalides, aryl dihalides are potential source of active halogen atoms and radicals in the upper atmosphere and ocean water[1] due to their strong absorption in the UV region. In the upper atmosphere the halogen radical reactions play an important role in depleting the ozone layer.[2] Therefore, studying and understanding halogen radical production in the gas phase, from the photolysis of various halogen containing compounds, remain active areas of research.

The photodissociation dynamics of aryl halides in the ultraviolet has been studied over the past 25 years starting with the pioneering work by Bersohn and co-workers.[3−5] Specifically, the dissociation of iodobenezene[6−10] and chlorobenzene[11−15] in the ultraviolet has been studied extensively. It has been established that the mechanism of photodissociation of aryl halides are qualitatively different from that of alkyl halides. Unlike in alkyl iodides where the excitation in the 200−305 nm region is localized on the C−I bond (σ*(C−I) ← n(I) transition) and the dissociation is direct, the predominant part of halobenzene dissociation is indirect and involves the $\pi^* \leftarrow \pi$, $\sigma^* \leftarrow \pi$ and $\pi^* \leftarrow$ n transitions localized on the aromatic ring. All the six transitions ($^1B_{2u}(S_1) \leftarrow {}^1A_{1g}(S_0)$, $^1B_{1u}(S_2) \leftarrow {}^1A_{1g}(S_0)$, $^1E_{1u}(S_3) \leftarrow {}^1A_{1g}(S_0)$, $^3B_{1u}(T_1) \leftarrow {}^1A_{1g}(S_0)$, $^3E_{1u}(T_2) \leftarrow {}^1A_{1g}(S_0)$ and $^3B_{2u}(T_3) \leftarrow {}^1A_{1g}(S_0)$) in benzene[16] are also seen in iodobenzene. However, when fluorine atom is substituted in the place of iodine atom, the $T_2 \leftarrow S_0$ band disappears and a new singlet−singlet transition around 230 nm appears.[17,18] In general, substitution of hydrogen atoms by fluorine or other halogen atoms alters (stabilizes) both the π and σ molecular orbitals of benzene.

Reports on aryl dihalides and mixed halide systems are not many although photodissociation of pentafluoroiodoiodobenzene has been studied in detail.[8,10] In their initial time-of-flight (TOF) dissociation studies Bersohn and co-workers[3−5] investigated many diiodoaromatics in the ultraviolet region. They concluded that a small fraction of the available energy is disposed in translation of the product fragments and the dissociation time scale is on the order of 1 ps. Later Nishi and co-workers studied the dissociation mechanism of *o*-, *m*-, and *p*-dichlorobenzene at 193 nm using the TOF technique.[19] They observed, in agreement with Bersohn's earlier work, that less than half of the available energy goes into product translation. They also observed three peaks in the TOF signals from the Cl atom and assigned the peaks to three different dissociation mechanisms. Using polarized light to decompose signals from various transitions, they concluded that the three different dissociation channels are (1) a fast direct dissociation channel through the repulsive σ* state, (2) an indirect predissociation channel via the triplet excited state, and (3) another rather slow predissociation channel through the highly excited vibrational levels close to the dissociation level of the ground state potential energy surface. For the isomers of dichlorobenzene, they predicted that the three channels are equally probable like in chlorobenzene,[14] and no significant change was caused by the additional chlorine atom. They also speculated that Cl* production would be a minor process in the dissociation. A later report on *o*-dichlorobenzene photodissociation at 266 nm by Zhu et al.[20] corroborated the results of Nishi and co-workers at 193 nm.

In this paper, we have investigated *o*-, *m*-, and *p*-chloroiodobenzenes along with iodobenzene and chlorobenzene at four different ultraviolet wavelengths (222, 236, 266, 280 nm) and probed the relative quantum yields of I* and Cl* production directly. Two different resonance enhanced multiphoton ionization (REMPI) schemes have been employed to detect iodine[21,22]

[†] Part of the special issue "Richard Bersohn Memorial Issue".

* Corresponding author. Email: pkdas@ipc.iisc.ernet.in. Fax: 91-80-23601552. Telephone: 91-80-22932662.

10.1021/jp049345k CCC: $27.50

and chlorine[23,24] atom fragments in the ground ($^2P_{3/2}$) as well as excited ($^2P_{1/2}$) states. The C−Cl bond dissociation energy is 97 kcal/mol in dichlorobenzene and the C−I bond dissociation energy is 64 kcal/mol in iodobenzene. Assuming that the C−Cl and C−I bond energies in chloroiodobenzenes will be similar to those in dichlorobenzene and iodobenzene, respectively, all four channels shown below

$$\begin{aligned} ClC_6H_4{-}I &\rightarrow ClC_6H_4 + I/I^* \\ &\rightarrow IC_6H_4 + Cl/Cl^* \end{aligned}$$

are accessible at the photon energies employed in our experiments. Further dissociation of C_6H_4X via the initial single photon excitation is not energetically possible in the near-ultraviolet. The basis of selecting these molecules is that, if there is any effect of the chlorine (iodine) atom on the dissociation mechanism (dynamics) of the other carbon−halogen bond, it will be more pronounced in these examples. The difference in electron affinity and size of the chlorine atom is much larger than that of the iodine atom and the interhalogen interaction is expected to change in going from the para isomer to the ortho isomer. The interatomic interaction between the two halogen atoms may occur via induced dipole−induced dipole or quadrupole−quadrupole interaction through space when they are situated close to each other as in the ortho configuration, and this may alter the exit channel dynamics of bond dissociation.

2. Experiment

The experimental setup has been described in detail elsewhere.[25] In brief, the photodissociation experiments were carried out inside a stainless steel chamber, evacuated continuously by a diffusion pump backed by a rotary pump to a base pressure of 10^{-6} Torr. A constant sample pressure between 200 and 400 μTorr was maintained for I and I* detection and 50−800 μTorr for Cl/Cl* detection. The pump and probe laser beams were aligned perpendicular to each other at the center of the chamber between two electrodes (2.5 × 2.5 cm^2 and 0.5 mm thick stainless steel plates) for the I atom detection. For the chlorine atom detection, we aligned the pump and the probe lasers parallel (counterpropagating) to each other. The delay between the pump and probe lasers was maintained between 50 and 100 ns. The pump and probe laser wavelengths were generated by various frequency doubling and mixing schemes described in a previous paper.[25] The probe beam was focused using a short focal length (5-in. fused silica) lens and the pump beam was contracted (0.5 cm dia) by a long focal length (typically 1 m f.l.) lens The iodine and chlorine atoms in the ground ($^2P_{3/2}$) and excited ($^2P_{1/2}$) states produced in the photolysis were detected by two different REMPI schemes.[21,23] The anode was maintained at +200 V and the voltage drop at the cathode across a 1 MΩ/1 W resistor to the ground was taken as signal. The output from the ion detector was collected through a homemade electrometer, amplified (typically 25 times), averaged over 50 shots, and digitized in a digital storage oscilloscope. The pump laser polarization was kept unchanged since, in our experiments, iodine and chlorine atoms are detected which are spherically symmetric and their recoil direction with the rotation of the pump laser polarization should not influence the REMPI signal intensity. All the compounds were purchased from Aldrich and were fractionally distilled prior to each experiment. The absorption spectra of *o*-, *m*-, and *p*-C_6H_4ICl along with C_6H_5Cl, and C_6H_5I in the ultraviolet were recorded in cyclohexane in a BECKMAN DU-600 spectrometer (Figure 1).

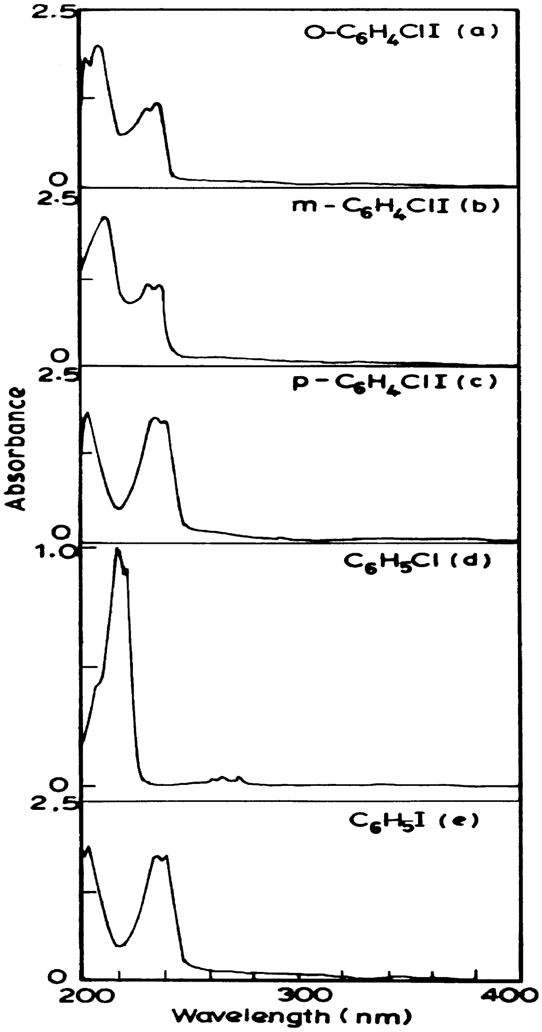

Figure 1. Absorption spectra of *o*-, *m*-, and *p*-C_6H_4ICl along with C_6H_5I and C_6H_5Cl in cyclohexane.

TABLE 1: ϕ^*(I) at Various Photolysis Wavelengths from Different Compounds[a]

compounds	280 nm	266 nm	236 nm	222 nm
o-C_6H_4ICl	0.69 ± 0.02	0.78 ± 0.02	0.54 ± 0.01	0.73 ± 0.02
m-C_6H_4ICl	0.67 ± 0.005	0.77 ± 0.02	0.63 ± 0.01	0.72 ± 0.04
p-C_6H_4ICl	0.57 ± 0.03	0.65 ± 0.01	0.33 ± 0.01	0.65 ± 0.01
C_6H_5I	0.58 ± 0.01	0.51 ± 0.01	0.59 ± 0.01	0.62 ± 0.02

[a] The errors shown in the table are statistical errors obtained from, at least, three measurements.

3. Results and Discussion

The REMPI spectra for I, I* and Cl, Cl* were recorded by scanning the probe laser across the (2+1) ionization lines of I (304.67 nm), I* (304.02 nm),[21] Cl (235.34 nm), and Cl* (235.21 nm).[23] The relative quantum yield of spin−orbit excited halogen atom, $\phi^* = N^*/(N + N^*)$, where N is the concentration of the nascent spin−orbit state and * refers to the excited state, were calculated from the REMPI signal intensities and are listed in Table 1 and Table 2, for I* and Cl*, respectively. The measured REMPI signal intensities S and S* may be expressed as

$$\frac{N^*}{N} = \frac{S^*}{S}\frac{F}{F^*} \tag{1}$$

where F contains various factors such as ionization cross section of the fragments, collection efficiency of the ions, and absorption cross section of the molecule at the probe REMPI wavelengths.[25]

TABLE 2: Relative ϕ*(Cl) at Various Photolysis Wavelengths from Different Compounds[a]

compounds	280 nm	266 nm	235 nm	222 nm
o-C_6H_4ICl	0.16 ± 0.02	0.57 ± 0.02	0.28 ± 0.01	0.36 ± 0.02
m-C_6H_4ICl	0.21 ± 0.02	0.33 ± 0.02	0.23 ± 0.01	0.35 ± 0.01
p- C_6H_4ICl	ND[b]	ND	0.25 ± 0.01	0.32 ± 0.02
C_6H_5Cl	ND	0.39 ± 0.01	0.14 ± 0.01	0.24 ± 0.02

[a] The errors shown in the table are statistical errors obtained from, at least, three measurements. [b] ND indicates undetectable Cl and Cl* signals from the photodissociation

We evaluated the ratio $f = F/F^*$ for I and I* using I_2 photolysis process[26] at 304.67 and 304.2 nm in our apparatus, which should yield equal amounts of I and I*. We found the value of $f = 1.00 \pm 0.05$ which is close to the expected value and the value of 0.90 reported by Eppink et al.[22] We have taken f as 1.0 and the quantum yield at various wavelengths were determined directly from I and I* REMPI signals.

For the Cl* quantum yield determination from REMPI signal intensities, the factor f has been revised several times in the literature. Initially Kawasaki et al.[27] used the value of $f = 1$, using two photon transitions, $4p^2D_{3/2} \leftarrow 3p^2P_{3/2}$ (235.336 nm) and $4p^2D_{3/2} \leftarrow 3p^2P_{1/2}$ (237.808 nm) albeit different frequencies from ours, to detect chlorine atoms by a (2 + 1) REMPI scheme. This was later modified by Gordon and co-workers[24] as 0.85 ± 0.10 to find an agreement between statistical and measured Cl* quantum yields in HCl. Since we use the same REMPI probe wavelengths used by Gordon et al.,[23] our natural choice for f would have been the same. However, in a recent measurement of this factor f, Regan et al.[28] have recommended a value of 1.06 ± 0.17 for the REMPI signal calibration of Cl and Cl* at the same REMPI probe wavelengths. The large error in the calibration is due to propagation of errors as ascribed by the authors. For our relative quantum yield measurement we have chosen the value of $f = 1.06$, and the error in the data reported in the two tables is the statistical error obtained from three or more separate measurements on different days.

The main objectives of this study are to find out (i) whether the photolysis of the mixed haloaryl compounds yield similar amounts of the spin−orbit excited halogen atoms compared to the corresponding monohalide compounds and (ii) how much influence does a halogen atom exert on the yield and formation of the other halogen atom in the excited state, specifically, when they occupy neighboring positions.

From the previous reports on the dihalobenzene dissociation,[3−5,19−20] it is clear that there are three pathways for dissociation of these molecules in the ultraviolet. The initial excitation takes the molecule to a one photon allowed state from the ground state. Three such transitions are possible of which two transitions are of $\sigma^* \leftarrow n$ type centered on the two carbon−halogen bonds and the third transition of $\pi^* \leftarrow \pi$ type localized on the aromatic core. The $\sigma^* \leftarrow n$ transition originating from the iodine 5p electrons of the C−I bond is weak and occurs with a peak absorption at ∼260 nm with a fwhm of ∼50 nm. The $\sigma^* \leftarrow n$ transition originating from the chlorine 3p electrons of the C−Cl bond is also weak but takes place at a much shorter wavelength at 174 nm with a fwhm of ∼10 nm. The $\pi^* \leftarrow \pi$ transition of the aromatic ring electrons occur at ∼ 235 nm with a fwhm of 20 nm. All these transitions are broad, and therefore, at any given ultraviolet wavelength, it is possible to access all or any combination of these transitions. Each of these transitions can further be decomposed to many more pure transitions. For example, underlying the $\sigma^* \leftarrow n$ transition localized on the C−X bond there are three transitions $^3Q_1 \leftarrow n$, $^3Q_0 \leftarrow n$, and $^1Q_1 \leftarrow n$ in increasing order of energy, as shown in the case of simple alkyl halides.[29,30] All these three transitions lead to direct dissociation pathways and only the $^3Q_0 \leftarrow n$ transition produces spin−orbit excited halogen atom. All the other three states including the ground state, that is, $^3Q_1$, $^1Q_1$, and n states correlate asymptotically to the ground-state halogen atom product. Of the six $\pi^* \leftarrow \pi$ type aromatic transitions mentioned earlier, only four transitions ($S_1 \leftarrow S_0$, $T_3 \leftarrow S_0$, $T_2 \leftarrow S_0$, $S_2 \leftarrow S_0$) are accessible in the 210−300 nm region.[10] On the basis of the selection rules for one photon transition, only excitations of the type $S_1/S_2 \leftarrow S_0$ will carry most of the transition strength in the wavelengths used in this study. Both the singlet excited states, S_1 and S_2, are bound states, and they cross the σ^*(C−X) states to dissociate into products. Therefore, excitation to the ring aromatic states in halobenzenes leads to indirect dissociation via the triplet $\sigma^* \leftarrow n$ states. This intersystem crossing is induced by spin−orbit interaction as well as a vibrational mode that helps symmetry breaking at the crossing region. In another competitive relaxation pathway, a fraction of the excited singlet molecules may undergo internal conversion to highly excited vibrational levels of the ground electronic state and predissociate. All these three mechanisms have more or less equal probability (∼$^1/_3$) of occurrence in dichlorobenzene as put forward earlier by Nishi and co-workers.[19] In the following sections, we discuss separately the differences observed in the I* and Cl* quantum yields in the *o*-, *m*-, and *p*-chloroiodobenzenes.

A. I* Quantum Yield. From Table 1 it is clear that ϕ*(I) for all the chloroiodobenzenes is more than 0.5 in all cases except *p*-chloroiodobenzene at 236 nm. In other words, more than 50% of the product iodine atoms are produced in their spin−orbit excited state. This implies that, regardless of the nature of the initially prepared excited state, the final state from which the molecules dissociate correlates to the excited state iodine atom. Only a minor fraction of the molecules dissociate to produce the ground state iodine atom. Generally, we would expect the relative I* yield to depend on (i) the electronic character of the initial excited state(s), (ii) the extent of intersystem crossing between the initially excited state and the final state from which the molecule dissociate, and (iii) the exit channel effects. With a few exceptions, the I* quantum yield in chloroiodobenzenes is, in general, higher than that in iodobenzene. While the exceptions point out the complex nature of the dissociation, the data in Table 1 bring out the effect of the chlorine atom on the production of I*($^2P_{1/2}$) quantum state in the dissociation. Two distinct effects are possibly exerted by the chlorine atom to influence the dynamics of C−I bond breaking in the excited state: (i) the reorganization of the $\pi^* \leftarrow \pi$ transition energy and (ii) the through space induced dipole-induced dipole and quadrupole−quadrupole interactions with the iodine atom (an exit channel effect). The first effect has been realized from the absorption spectra of C_6H_5I and C_6H_5Cl (Figure 1), and it is clear that there is a 8 nm red shift (from 257 to 265 nm) of the $\pi^* \leftarrow \pi$ transition due to the presence of chlorine atom in the ring. The shift indicates that the chlorine atom stabilizes the π^* antibonding orbital more than the π bonding orbital. In the F atom substitution study on the I* quantum yield in alkyl[31]as well as aryl iodides,[8,10] the spin−orbit interaction effects exerted by the F atom have been recognized. In the direct dissociation mechanism, the additional halogen atom (chlorine atom in the present context) increases the singlet−triplet energy gap in the intersystem crossing region and thus forces most of the molecules to dissociate from the excited state which correlates to the I* product. The influence is much more complex in the indirect dissociation mechanism as discussed earlier by Kavita et al.[10] in the case of pentaflu-

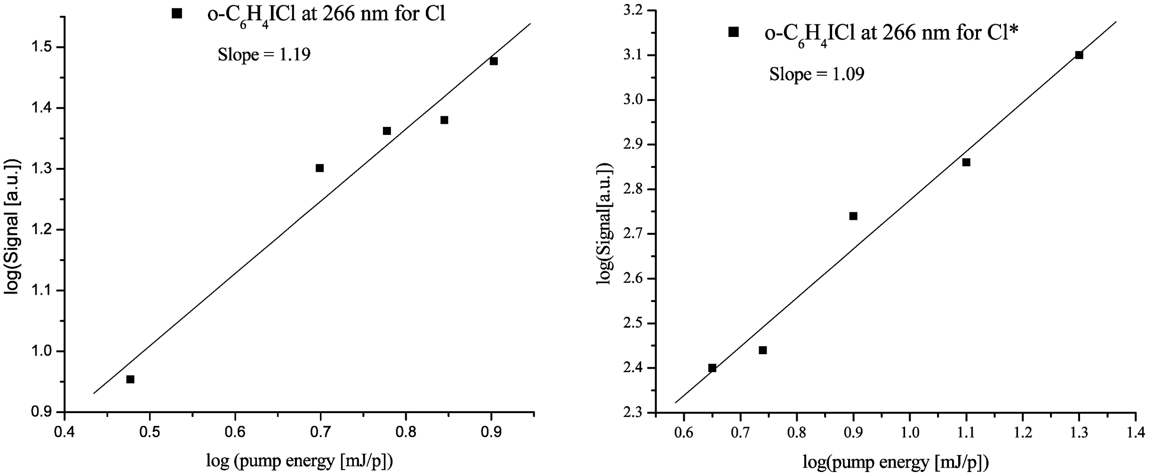

Figure 2. Pump laser power dependence of Cl/Cl* REMPI signal from o−C_6H_4ICl. The straight line is a linear least-squares fit through the experimental points. The slope of the lines is mentioned inside the plots.

oroiodobenzene. Also the influence is stronger if the halogen atom is attached to the carbon atom holding the C−I bond or the number of halogen atom substitutions in the molecule is high. In the example of chloroiodobenzene, only one halogen atom is attached to the next nearest carbon atom. Then why is there a significant variation in I* yield from iodobenzene to *o*-chloroiodobenzene in many cases? The spin−orbit interaction exerted by the lone Cl atom alone cannot account for such a large change. If we look at the electron affinity of the chlorine atom, it is 3.617 eV, which is large. This may in turn exhibit a negative inductive effect (−I effect) on the carbon atoms in the ortho and para positions and reduce the electron density on those carbon atoms. On this basis alone, we would expect the *o*- and *p*-chloroiodobenzene to produce more or less equal amounts of I* atoms in the photolysis and *m*-chloroiodobenzene which is not affected by the −I effect to exhbit similar quantum yield to that of iodobenzene. However, the fact that the I* quantum yield is much higher in the ortho compound than in the para indicates that the −I effect exerted by the chlorine atom cannot be the only factor affecting the dynamics at the exit channel. If we look at the optimized geometry of the ortho, meta, and para isomers using LanL2DZ basis set within the Gaussian-98 set of programs, we find that the shortest distances between the Cl and I atoms in the ground state are 3.485 Å for the ortho, 5.833 Å for the meta, and 6.751 Å for the para compounds. The distance in the *o*-chloroiodobenzene is very much within the van der Waals distance of the two atoms (the sum of the mean van der Waals radii of Cl and I atoms,[32] respectively, is (1.98 + 1.75Å) or 3.73 Å), and, thus the electronic interaction between the two atoms through space is expected to be large. The distances are unlikely to change very much in the excited states from which the molecule dissociates. In fact, both the halogen atoms have large quadrupole moments, and they can interact strongly through quadrupole−quadrupole interaction apart from the induced dipole−induced dipole (both the C−Cl and C−I bonds have dipole moments) interaction. All these exit channel interactions perhaps give greater I* production through the direct dissociation pathway. This interaction will also help the indirect pathway for I* production by mixing the π^* states with the dissociative state(s) by providing higher density of states in the interaction region. Since the separation distance between the two halogen atoms follow the order *o*- < *m*- < *p*-, the I* quantum yield at a given wavelength is expected to follow the reverse order; that is *o*- > *m*- > *p*-. What is observed is more like *o*- > *m*- ≥ *p*- since the difference in the quantum yields between meta and para isomers are marginally different. However, the reason for the deviation of the quantum yield data at 236 nm for *p*-chloroiodobenzene (ϕ^*(I) = 0.33) from the general trend observed in this study is not at all obvious.

B. Cl* Quantum Yield. It is natural to think that the contribution from the $\sigma^* \leftarrow n$ transition localized on C−Cl chromophore which peaks at ∼170−180 nm will be insignificant in the photodissociation at all the dissociation wavelengths employed in this study, and consequently no Cl/Cl* will be produced in the near-ultraviolet dissociation of C_6H_4ICl. However, the most exciting observation in this study is that all of the compounds produce Cl* fragments in a measurable quantity at most of the wavelengths of investigation. This is not surprising energetically since it is possible to produce both Cl and Cl* atoms in a single photon excitation process at the wavelengths chosen here. In fact, the threshold for Cl/Cl* production in wavelength is ∼295 nm, and this has been verified by trying to dissociate chloroiodobenzene at ∼304 nm. No Cl/Cl* was detected at ∼304 nm. A laser power dependence study show that the production of Cl/Cl* is unlikely to be originated via a two-photon process (Figure 2). We rule out, first, the dissociation of the C−I bond followed by a further dissociation of the chloroaryl radical, that is, a secondary dissociation pathway for the production of Cl/Cl*. The energy of a single photon in the wavelength range 222−280 nm is sufficient to break the C−Cl bond and produce either Cl or Cl* atoms. Table 2 lists the Cl* quantum yield, ϕ^*(Cl), for all the compounds (C_6H_5Cl, and isomers of C_6H_4ICl) at various photolysis wavelengths. For chlorine atom detection, the pump wavelength of 236 nm was not used; instead, photons from the same probe laser at ∼235 nm were used for dissociation as well as detection. The relative quantum yields in Table 2 are less than 0.5 with the exception of *o*-C_6H_4ICl. In most cases, more than 50% of the product chlorine atoms are produced in the spin−orbit ground state. This is in sharp contrast to what has been observed for the I* production as discussed above. The quantum yield of Cl* production in chloroiodobenzenes is higher than that of chlorobenzene at all wavelengths except for *m*-C_6H_4ICl at 266 nm. With this exception, the measured Cl* quantum yields reveal the effect of the neighboring iodine atom on the dynamics of the C−Cl bond rupture in much the same way as does the chlorine atom influence the I* yield.

The reason for the production of less Cl* at longer wavelengths can be speculated. Since the σ^*(C−Cl) ← n(Cl) transition centered on the C−Cl bond is much higher in energy, and therefore, the direct dissociation pathway via the C−Cl bond

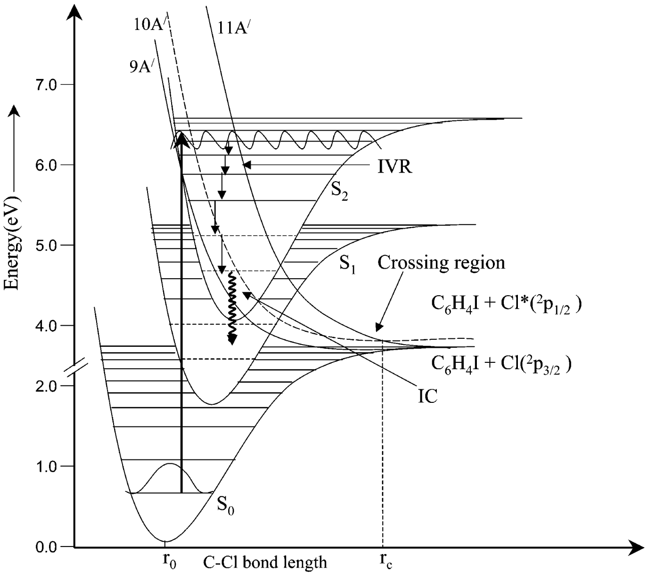

Figure 3. Schematic potential energy diagram describing the mechanism of the C−Cl bond dissociation. IVR is intramolecular vibrational relaxation, and IC, internal conversion. Under C_s geometry, 9A′, 10A′, and 11A′ are the (σ^*(C−Cl) ← n(Cl)) transitions.

excitation is not available for the Cl/Cl* production. However, the two indirect pathways as applicable to the C−I bond dissociation are accessible. The Cl* atoms are then produced by a curve crossing mechanism from the initially excited S_1/S_2 ← S_0 state (s) via the dissociative state(s). Observation of a low ϕ^*(Cl) indicates that this curve crossing must be hindered. Since the initially prepared excited state is low in energy compared to the σ^*(C−Cl) ← n(Cl) states, the intersystem curve crossing must be taking place at a much larger C−Cl bond distance allowing the molecules to spend a long time in the exit channel and dissociate by forming Cl atoms in the ground spin−orbit state. This has been shown in a schematic potential energy diagram in Figure 3. In this diagram, a molecule excited to the S_2 state first undergoes intramolecular vibrational relaxation (IVR) to lower vibrational energy levels of the excited state. A fraction of the molecules then crosses over to the dissociative states to produce both Cl* and Cl products. A small fraction of the molecules can also undergo fast internal conversion to the high vibrational levels of the S_0 state which will eventually dissociate and produce ground-state Cl atom. Also in this case, the ortho effect on ϕ^*(Cl) is much more prominent. The variation of ϕ^*(Cl) as a function of wavelength has to do with the extent to which the various initial excitation carry the total transition strength and how the final repulsive states are placed with respect to the initial excited states. In other words, the variation reflects the actual dynamics of the dissociation from the excited-state potential energy surfaces.

4. Concluding Remarks

From I* and Cl* quantum yield measurements in the photolysis of *o*-, *m*-, and *p*-chloroiodobenzenes in the ultraviolet, we have shown, in this paper, that both chlorine and iodine atoms are produced in their spin−orbit excited as well as ground states. The dynamics of spin−orbit excited halogen atom production is very complex and depends on (i) the electronic nature of the initially prepared state, (ii) the intersystem crossing, and (iii) the exit channel dynamics. While, in the case of the C−I bond rupture, three competitive pathways (one direct and two indirect) for dissociation are available, for the C−Cl bond scission only two indirect paths are possible. The absence of the direct excitation pathway in the latter results in a low yield of Cl*. Among the three isomers of chloroiodobenzene, the ortho compound produces maximum amounts of Cl* and I*, indicating stronger coupling between various photodissociation pathways in the exit channel. The coupling is, perhaps, aided by through space induced dipole-induced dipole and/or quadrupole−quadrupole interactions between the two halogen atoms. A quantitative dynamics calculation using accurate potential energy surfaces is necessary for developing a more quantitative understanding of the ultraviolet dissociation of mixeddihalo benzenes.

Acknowledgment. We thank Prof. A. G. Menon for helping us with the design of the REMPI detector. The research described here has been funded generously by the Department of Atomic Energy, Government of India.

References and Notes

(1) Vogt, R.; Sander, R.; Glasow, R. V.; Crutzen, P. J. *J. Atmos. Chem.* **1999**, *32*, 375.

(2) Dubtsov, S. N.; Skubnevskaya, G. I.; Kutzenogii, K. P. *J. Aerosol Sci.* **1991**, *23*, 181.

(3) Dzvonik, M.; Yang, S.; Bersohn, R. *J. Chem. Phys.* **1974**, *61*, 4408.

(4) Kawasaki, M.; Lee, S. J.; Bersohn, R. *J. Chem. Phys.* **1977**, *66*, 2647.

(5) Freedman, A.; Yang, S. C.; Kawasaki, M.; Bersohn, R. *J. Chem. Phys.* **1980**, *72*, 1028.

(6) Freitas, J. E.; Hwang, H. J.; El-Sayed, M. A. *J. Phys. Chem.* **1993**, *97*, 12481.

(7) Cheng. P. Y.; Zhong, D.; Zewail, A. H. *Chem. Phys. Lett.* **1995**, *237*, 399.

(8) Griffiths, J. A.; Jung, K. W.; El-Sayed, M. A. *J. Phys. Chem.* **1996**, *100*, 7989.

(9) Unny, S.; Du, Y.; Zhu, L.; Truhins, K.; Gordon, R. J.; Sugita, A.; Kawasaki, M.; Matsumi, Y.; Delmdahl, R.; Parker, D. H.; Berces, A. *J. Phys. Chem. A* **2001**, *105*, 2270.

(10) Kavita, K.; Das, P. K. *J. Chem. Phys.* **2002**, *117*, 2038.

(11) Ichimura, T.; Mori, Y.; Shinohara, H.; Nishi, N. *Chem. Phys. Lett.* **1985**, *122*, 51.

(12) Ichimura, T.; Mori, Y.; Shinohara, H.; Nishi, N. *Chem. Phys. Lett.* **1985**, *122*, 55.

(13) Satyapal, S.; Tasaki, S.; Bersohn, R. *Chem. Phys. Lett.* **1993**, *203*, 349.

(14) Ichimura, T.; Mori, Y.; Shinohara, H.; Nishi, N. *Chem. Phys.* **1994**, *189*, 117.

(15) Wang, G.; Zhu, R.; Zhang, H.; Han, K.-L.; He, G.-Z.; Lou, N.-Q. *Chem. Phys. Lett.* **1998**, *288*, 429.

(16) Doering, J. P. *J. Chem. Phys.* **1977**, *67*, 4065.

(17) Frueholz, R. P.; Flicker, W. M.; Mosher, O. A.; Kupperman, A. *J. Chem. Phys.* **1979**, *70*, 3057.

(18) Trudell, B. C.; Price, S. J. W. *Can. J. Chem.* **1979**, *57*, 2256.

(19) Ichimura, T.; Mori, Y.; Shinohara, H.; Nishi, N. *J. Chem. Phys.* **1997**, *107*, 835.

(20) Zhu, R.-S.; Zhang, H.; Wang, G.-J.; Gu, X.-B.; Han, K.-L.; He, G.-Z.; Lou, N.-Q. *Chem. Phys.* **1999**, *248*, 285.

(21) Gedanken, A.; Robin, M. B.; Yafet, Y. *J. Chem. Phys.* **1982**, *76*, 4798.

(22) Eppink, A. T. J. B.; Parker, D. H. *J. Chem. Phys.* **1998**, *109*, 4758.

(23) Arepalli, S.; Presser, N.; Robie, D.; Gordon, R. J. *Chem. Phys. Lett.* **1985**, *118*, 88.

(24) Liyanage, R.; Yang, Y.; Hashimoto, S.; Gordon, R. J.; Field, R. W. *J. Chem. Phys.* **1995**, *103*, 6811.

(25) Senapati, D.; Kavita, K.; Das, P. K. *J. Phys. Chem. A* **2002**, *106*, 8479.

(26) Hwang, H. J.; El-Sayed, M. A. *J. Phys. Chem.* **1991**, *95*, 8044.

(27) Matsumi, Y.; Tonokura, K.; Kawasaki, M.; Inoue, G.; Satyapal, S.; Bersohn, R. *J. Chem. Phys.* **1991**, *94*, 2669.

(28) Regan, P. M.; Langford, S. R.; Ascenzi, D.; Cook, P. A.; Orr-Ewing, A. J.; Ashfold, M. N. R. *Phys. Chem. Chem. Phys.* **1999**, *1*, 3247.

(29) Gedanken, A.; Rowe, M. D. *Chem. Phys. Lett.* **1975**, *34*, 39.

(30) Phillips, D. L. *Prog. React. Kinet. Mech.* **1999**, *24*, 223 and references therein.

(31) Kavita, K.; Das, P. K. *J. Chem. Phys.* **2000**, *112*, 8426.

(32) Bondi, A. *J. Phys. Chem.* **1964**, *68*, 441.